Continuum Mech. Thermodyn.
DOI 10.1007/s00161-010-0155-8

ORIGINAL ARTICLE

**J. Arghavani · F. Auricchio · R. Naghdabadi · A. Reali ·
S. Sohrabpour**

A 3D finite strain phenomenological constitutive model for shape memory alloys considering martensite reorientation

Received: 30 November 2009 / Accepted: 4 June 2010

Abstract Most devices based on shape memory alloys experience both finite deformations and non-proportional loading conditions in engineering applications. This motivates the development of constitutive models considering finite strain as well as martensite variant reorientation. To this end, in the present article, based on the principles of continuum thermodynamics with internal variables, a three-dimensional finite strain phenomenological constitutive model is proposed taking its basis from the recent model in the small strain regime proposed by Panico and Brinson (J Mech Phys Solids 55:2491–2511, 2007). In the finite strain constitutive model derivation, a multiplicative decomposition of the deformation gradient into elastic and inelastic parts, together with an additive decomposition of the inelastic strain rate tensor into transformation and reorientation parts is adopted. Moreover, it is shown that, when linearized, the proposed model reduces exactly to the original small strain model.

Keywords Shape memory alloys · Finite strain · Phase transformation · Constitutive model · Reorientation · Non-proportional loading

1 Introduction

Smart materials are well-known materials exhibiting special properties, known as pseudo-elasticity (or superelasticity), one-way and two-way shape memory effects [1,2], suitable for industrial applications and

Communicated by Prof. Thomas Pence.

J. Arghavani · R. Naghdabadi (✉) · S. Sohrabpour
Department of Mechanical Engineering, Sharif University of Technology, 11155-9567 Tehran, Iran
E-mail: naghdabd@sharif.edu

J. Arghavani · F. Auricchio · A. Reali
Dipartimento di Meccanica Strutturale, Università degli Studi di Pavia, Pavia, Italy

F. Auricchio
Center for Advanced Numerical Simulation (CeSNA), IUSS, Pavia, Italy

F. Auricchio · A. Reali
European Centre for Training and Research in Earthquake Engineering (EUCENTRE), Pavia, Italy

R. Naghdabadi
Institute for Nano-Science and Technology, Sharif University of Technology, 11155-9567 Tehran, Iran

S. Sohrabpour
Department of Engineering Sciences, The Academy of Sciences of IR Iran, Tehran, Iran

Published online: 03 July 2010

engineering. The interest in the mechanical behavior of SMAs is rapidly growing with the increasing number of potential industrial applications. Early commercialization activities, fueled by applications such as rivets, heat engines, couplings, circuit breakers and automobile actuators, started in the 1970s, were intense and often highly secretive [3]. However, in the last decades, the knowledge of SMAs has progressively spread out more and more, up to the fact that nowadays pseudo-elastic Nitinol is a common and well-known engineering material in the medical industry [4,5].

The origin of SMA features is a reversible thermo-elastic martensitic phase transformation between a high symmetry, austenitic phase and a low symmetry, martensitic phase. Austenite is a solid phase, usually characterized by a body-centered cubic crystallographic structure, which transforms into martensite by means of a lattice shearing mechanism. When the transformation is driven by a temperature decrease, martensite variants compensate each other, resulting in no macroscopic deformation. However, when the transformation is driven by the application of a load, specific martensite variants, favorable to the applied stress, are preferentially formed, exhibiting a macroscopic shape change in the direction of the applied stress. Upon unloading or heating, this shape change disappears through the reversible conversion of the martensite variants into the parent phase [1,6].

The starting and finishing temperatures of a stress-free SMA during forward transformation (austenite to martensite), M_s and M_f, as well as the starting and finishing temperatures during reverse transformation, A_s and A_f, are the four characteristic temperatures for a shape memory alloy. In a stress-free condition, at a temperature above A_f, only austenitic phase is stable, while martensite is stable only at a temperature below M_f. Applying a stress at a temperature above A_f, SMAs exhibit pseudo-elastic behavior with a full recovery of inelastic strain upon unloading. Instead, at a temperature below A_s, the material presents the shape memory effect with permanent inelastic strains upon unloading, which may be recovered by heating.

In most applications, SMAs experience general thermo-mechanical loads, which are more complicated than uniaxial or multiaxial proportional loadings, and typically undergo large rotations and moderate strains (i.e. in the range of 10% for polycrystals) [1]. For example, with reference to biomedical applications, stent structures are usually designed to significantly reduce their diameter during the insertion into a catheter; thereby, large rotations combined with moderate strains occur and the use of a finite deformation scheme is preferred.

Several experimental studies show that the so-called variant reorientation can be assumed as the main phenomenon in non-proportional loadings of SMAs [7–12]. Recently, Grabe and Bruhns [12] have conducted several multiaxial experiments on polycrystalline NiTi within a wide temperature range, showing the strong nonlinearity as well as the path dependencies of the response and highlighting the presence of reorientation processes for complex loading paths.

These experimental observations, as well as situations experienced by SMAs in real engineering applications, call for the development of a 3D SMA constitutive model, taking into account both finite strain and variant reorientation under general loading conditions (multiaxial non-proportional loadings).

Up to now, there have been several attempts to properly reproduce SMA features in a predictive modeling frame. The resulting models can be in general categorized as either micro, micro-macro or macro. Description of micro-scale features, such as nucleation, interface motion, twin growth, etc., is the main focus of micro models. They are useful to understand the fundamental phenomenon, although they are not easily applicable at the structural scale. Micro–macro studies combine micromechanics and macroscopic continuum mechanics to derive constitutive laws of the material. The predictions by these approaches are successful, but the time-consuming computations make them inappropriate for engineering applications. Phenomenological or macro approaches use the principles of continuum thermodynamics with internal variables to describe the material behavior and, in general, they are suitable for use within numerical methods, such as the finite element method (FEM), in an efficient way. A comprehensive list of references for micro- and macro-models can be found in Patoor et al. [13] and Lagoudas et al. [14], respectively. In this study, we focus on a phenomenological macro modelling approach, which is able only to give an average representation of the phenomena occurring at the material micro-mechanical level.

The majority of the current 3D macroscopic constitutive models of SMA have been developed in the pseudo-elastic range and small deformation regime [15–33]. Finite deformation SMA constitutive models available in the literature [9,34–43] have been mainly developed by extending small strain constitutive models. The approach in most of the cases is based on the multiplicative decomposition of the deformation gradient into an elastic and an inelastic or transformation part [9,34–40], although there are some models in the literature, which have utilized an additive decomposition of the strain rate tensor into an elastic and an inelastic part [42]. In the following, we mention some of the finite deformation SMA constitutive models currently available in the literature.

The model by Auricchio and Taylor [34] is apparently the first macroscopic SMA constitutive model taking into account finite deformation pseudo-elasticity. Disregarding the first invariant of stress, this model reduces to Raniecki and Lexcellent model (R_L model) [44] when linearized. Pethö [36] decomposes the total deformation gradient into elastic, plastic and phase transformation parts, describing elasticity using an integrable hypoelastic model based on the logarithmic rate.

Ziolkowski [37] extends a version of the R_L model [20,44] to the large deformation regime, considering thermo-mechanical coupling effects. A multiplicative decomposition of the deformation gradient is also proposed by Helm [9,26] and Reese and Christ [38,39]. Recently, Evangelista et al. [40] and Arghavani et al. [41] have extended the small strain model proposed by Souza et. al. [23] and discussed by Auricchio and Petrini [45] to the finite deformation regime. While all the above-mentioned references use a multiplicative decomposition of the deformation gradient, Müller and Bruhns [42] utilize an additive decomposition of the strain rate tensor into an elastic and a phase transformation part. In particular, they extend the R_L small strain model [20] to take into account finite deformations and finally reach a rate constitutive model in terms of the logarithmic spin tensor. Bernardini and Pence [43] have proposed a finite strain constitutive model within the framework of multifield theories. Also, some large strain non-phenomenological models have been proposed in the literature (see e.g., [46–52]).

As stated above, finite strain constitutive models are often based on successful small strain ones. Along this line, the recently proposed three-dimensional model by Panico and Brinson [21], based on the classical framework of thermodynamics of irreversible processes, represents a suitable candidate to be extended to the finite strain regime. In particular, this model is interesting for its capability to model both pseudo-elasticity and shape memory effect, as well as for its improved description of martensite reorientation under non-proportional loading conditions. Starting from this basis, the development of a finite deformation model, which is also capable to capture loading non-proportionality effects (as the main feature of the proposed constitutive model in this work compared with the available models in the literature), is the main goal of the present work and can be an important tool to predict SMA device behavior under complicated loading conditions. Therefore, in this work, a finite strain model based on [21] is presented.

The article is organized as follows. Section 2 briefly reviews the small strain model proposed in [21]. In Sect. 3 after presenting some preliminaries, we introduce the multiplicative decomposition of the deformation gradient into elastic and inelastic parts, the Helmholtz free energy function definition and an additive decomposition of the inelastic strain rate tensor into transformation and reorientation parts. We moreover derive the evolution equations, satisfying the Clausius–Duhem inequality form of the second law of thermodynamics, and we present the finite deformation constitutive model equations with respect to the reference configuration. In Sect. 4 we show that, when linearized, the developed constitutive model reduces to the original small strain one [21]. In Sect. 5, we compare the small (SSF) and finite strain formulations (FSF) under simple shear test. We finally draw conclusions in Sect. 6.

2 Review of the small strain constitutive model proposed by Panico and Brinson

In this section, we present the small strain constitutive model presented by Panico and Brinson [21], which will be extended in Sect. 3 to derive the finite deformation constitutive model. Such a model utilizes an additive decomposition of the total strain into an elastic and an inelastic (traceless) part, as usual in the case of small strains:

$$\boldsymbol{\varepsilon} = \boldsymbol{\varepsilon}^{\mathrm{e}} + \boldsymbol{\varepsilon}^{\mathrm{in}}. \tag{1}$$

The stress-induced martensite fraction, z_σ is then related to the inelastic strain as follows:

$$z_\sigma = \frac{\|\boldsymbol{\varepsilon}^{\mathrm{in}}\|}{\sqrt{\frac{3}{2}}\gamma} \tag{2}$$

where γ is the maximum uniaxial transformation strain and $\|\cdot\|$ is the norm operator, defined as $\|\boldsymbol{A}\| = (\boldsymbol{A} : \boldsymbol{A}^{\mathrm{T}})^{\frac{1}{2}}$[1], while $\boldsymbol{A} : \boldsymbol{B} = A_{ij}B_{ij}$. From (2), the rate of martensite volume fraction can be written as:

$$\dot{z}_\sigma = \frac{\boldsymbol{\varepsilon}^{\mathrm{in}} : \dot{\boldsymbol{\varepsilon}}^{\mathrm{in}}}{\sqrt{\frac{3}{2}}\gamma\,\|\boldsymbol{\varepsilon}^{\mathrm{in}}\|}. \tag{3}$$

It is assumed that the rate of inelastic strain is due to transformation of the parent phase and to reorientation of the previously developed oriented martensite, that is:

$$\dot{\boldsymbol{\varepsilon}}^{\mathrm{in}} = \dot{\boldsymbol{\varepsilon}}^{\mathrm{tr}} + \dot{\boldsymbol{\varepsilon}}^{\mathrm{re}} \tag{4}$$

where $\dot{\boldsymbol{\varepsilon}}^{\mathrm{tr}}$ and $\dot{\boldsymbol{\varepsilon}}^{\mathrm{re}}$ are the transformation and reorientation strain rate tensors, respectively.

Also, the total martensite fraction, z, is obtained as the sum of stress-induced and temperature-induced parts:

$$z = z_\sigma + z_{\mathrm{T}}, \quad 0 \le z \le 1, \quad 0 \le z_\sigma \le 1, \;\; 0 \le z_{\mathrm{T}} \le 1 \tag{5}$$

where z_{T} represents the temperature-induced martensite fraction.

Since, from a physical point of view, variant reorientation does not change the martensite volume fraction, the condition $\boldsymbol{\varepsilon}^{\mathrm{in}} : \dot{\boldsymbol{\varepsilon}}^{\mathrm{re}} = 0$ has to be imposed.[2] Then Eq. 3 becomes:

$$\dot{z}_\sigma = \frac{\boldsymbol{\varepsilon}^{\mathrm{in}} : \dot{\boldsymbol{\varepsilon}}^{\mathrm{tr}}}{\sqrt{\frac{3}{2}}\gamma\,\|\boldsymbol{\varepsilon}^{\mathrm{in}}\|}. \tag{6}$$

Considering stress-induced martensite fraction, z_σ, and temperature-induced martensite fraction, z_{T}, as internal variables together with $\boldsymbol{\varepsilon}^{\mathrm{e}}$ and T as control variables, the following classical expression for the Helmholtz free energy function of the three-phase system is adopted:

$$\begin{aligned}\psi(\boldsymbol{\varepsilon}^{\mathrm{e}}, T, z_\sigma, z_{\mathrm{T}}) = {} & \frac{1}{2\rho}\boldsymbol{\varepsilon}^{\mathrm{e}} : \mathbb{L} : \boldsymbol{\varepsilon}^{\mathrm{e}} + u_0^{\mathrm{A}} - T\eta_0^{\mathrm{A}} - z_{\mathrm{T}}\left(\Delta u_0 - T\Delta\eta_0\right) \\ & + z_\sigma \langle T\Delta\eta_0 - \Delta u_0\rangle + c_v\left[(T - T_0) - T\ln\left(\frac{T}{T_0}\right)\right] + \Delta\psi \end{aligned} \tag{7}$$

where ρ is the material density, $\mathbb{L}$ is the isotropic elasticity tensor assumed to be the same for all phases. The energy and entropy differences $\Delta u_0 = u_0^{\mathrm{A}} - u_0^{\mathrm{M}}$ and $\Delta\eta_0 = \eta_0^{\mathrm{A}} - \eta_0^{\mathrm{M}}$ have been adopted where u_0^{A} and u_0^{M} are the specific free energies of austenite and martensite, η_0^{A} and η_0^{M} are the specific entropies of austenite and martensite. Moreover, c_v is the specific heat at constant volume, T_0 is the equilibrium temperature between parent and product phase, $\Delta\psi$ is the so-called configurational energy originated by the phase mixture. The Macaulay brackets calculate the positive part of the argument, i.e., $\langle x\rangle = (x + |x|)/2$.
The configurational energy is assumed to depend only on z_σ according to the following quadratic form:

$$\Delta\psi = \frac{1}{2}H_\sigma z_\sigma^2 \tag{8}$$

where H_σ is a material parameter governing the initial hardening during the phase transformation.
The rest of the formulation follows standard arguments, so it is not reported here and the reader is referred to [21] for more details. The final form of the constitutive model is summarized as follows:

[1] We remark that the norm operator used in this work is different from the Frobenius norm (defined as $\|\boldsymbol{A}\| = (\boldsymbol{A} : \boldsymbol{A})^{\frac{1}{2}}$), but is an admissible operator and satisfies the objectivity requirement as it can be shown by using the transformation rule of second order tensors, i.e. $A_{ij}^* = Q_{ik}Q_{jl}A_{kl}$ ($\boldsymbol{Q}$ being a proper orthogonal tensor), to obtain:
$\boldsymbol{A}^* : \boldsymbol{A}^{*\mathrm{T}} = A_{ij}^*A_{ji}^* = Q_{ik}Q_{jl}A_{kl}Q_{jm}Q_{in}A_{mn} = (Q_{ik}Q_{in})(Q_{jl}Q_{jm})(A_{kl}A_{mn}) = \delta_{nk}\delta_{ml}A_{kl}A_{mn} = A_{kl}A_{lk} = \boldsymbol{A} : \boldsymbol{A}^{\mathrm{T}}$
Moreover, both norm definitions yield the same result for a symmetric tensor. Finally, the adopted norm has already been used in several works (see, e.g. [39]).

[2] We refer the reader to the recently published work by Arghavani et al. [22], which explains more clearly the physical concept of this constraint.

– Stress quantities

$$\begin{cases} \boldsymbol{\sigma} &= \mathbb{L} : \left(\boldsymbol{\varepsilon} - \boldsymbol{\varepsilon}^{\text{in}}\right) \\ \boldsymbol{x} &= \rho\left[\langle T\,\Delta\eta_0 - \Delta u_0\rangle + H_\sigma z_\sigma\right] \dfrac{\boldsymbol{\varepsilon}^{\text{in}}}{\sqrt{\frac{3}{2}}\gamma\,\|\boldsymbol{\varepsilon}^{\text{in}}\|} \\ \boldsymbol{x}_{\text{tr}} &= \boldsymbol{s} - \boldsymbol{x} \\ \boldsymbol{x}_{\text{re}} &= \boldsymbol{s} \\ x_{\text{T}} &= -\rho\,(T\,\Delta\eta_0 - \Delta u_0) \end{cases} \tag{9}$$

– Evolution equations

$$\begin{aligned} \dot{\boldsymbol{\varepsilon}}^{\text{in}} &= \dot{\lambda}_{\text{tr}}\boldsymbol{x}_{\text{tr}} + \dot{\lambda}_{\text{re}}\hat{\mathbb{I}} : \boldsymbol{x}_{\text{re}} \\ \dot{z}_{\text{T}} &= \dot{\lambda}_{\text{T}}\boldsymbol{x}_{\text{T}} \end{aligned} \tag{10}$$

– Limit functions

$$\begin{aligned} f_{\text{tr}} &= \|\boldsymbol{x}_{\text{tr}}\| - y_{\text{tr}}(z_\sigma) \\ f_{\text{re}} &= \tfrac{1}{2}\boldsymbol{x}_{\text{re}} : \hat{\mathbb{I}} : \boldsymbol{x}_{\text{re}} - y_{\text{re}} \\ f_{\text{T}} &= \begin{cases} x_T - y_{\text{T}}^f(z_{\text{T}}) & \text{if } \dot{z}_{\text{T}} > 0 \\ -x_T - y_{\text{T}}^r(z_{\text{T}}) & \text{if } \dot{z}_{\text{T}} < 0 \end{cases} \end{aligned} \tag{11}$$

– Kuhn–Tucker conditions

$$\begin{aligned} &f_{\text{tr}} \le 0, \quad \dot{\lambda}_{\text{tr}} \ge 0, \quad \dot{\lambda}_{\text{tr}} f_{\text{tr}} = 0 \\ &f_{\text{re}} \le 0, \quad \dot{\lambda}_{\text{re}} \ge 0, \quad \dot{\lambda}_{\text{re}} f_{\text{re}} = 0 \\ &f_{\text{T}} \le 0, \quad \dot{\lambda}_{\text{T}} \ge 0, \quad \dot{\lambda}_{\text{T}} f_{\text{T}} = 0 \end{aligned} \tag{12}$$

– Martensite volume fractions

$$z_\sigma = \frac{\|\boldsymbol{\varepsilon}^{\text{in}}\|}{\sqrt{\frac{3}{2}}\gamma}, \quad 0 \le z_\sigma \le 1, \;\; 0 \le z_{\text{T}} \le 1, \quad 0 \le z_{\text{T}} + z_\sigma \le 1 \tag{13}$$

In the equations above, $\boldsymbol{\sigma}$ is the Cauchy stress and $\boldsymbol{s} = \boldsymbol{\sigma} - \frac{1}{3}\text{tr}(\boldsymbol{\sigma})\mathbf{1}$ is the deviatoric stress, while the fourth-order tensor $\hat{\mathbb{I}}$ is defined as:

$$\hat{\mathbb{I}} = \mathbb{I} - \boldsymbol{h} \otimes \boldsymbol{h}, \quad \boldsymbol{h} = \frac{\boldsymbol{\varepsilon}^{\text{in}}}{\|\boldsymbol{\varepsilon}^{\text{in}}\|} \tag{14}$$

being $\mathbf{1}$ and $\mathbb{I}$ the second- and fourth-order identity tensors, respectively. Moreover, y_{re} is a material parameter, which controls the reorientation process, while $y_{\text{tr}}(z_\sigma)$ is a function that governs the kinematics of the phase transformation and is assumed to have the following form:

$$y_{\text{tr}}(z_\sigma) = \begin{cases} A^{\text{f}} z_\sigma - B^{\text{f}} z_\sigma \ln(1 - z_\sigma) + C^{\text{f}} & \text{if } \dot{z}_\sigma > 0 \\ A^{\text{r}}(1 - z_\sigma) - B^{\text{r}}(1 - z_\sigma)\ln(z_\sigma) + C^{\text{r}} & \text{if } \dot{z}_\sigma < 0 \end{cases} \tag{15}$$

with $A^{\text{f,r}},\ B^{\text{f,r}},\ C^{\text{f,r}}$ material parameters. Dependency of y_{tr} on the stress-induced martensite fraction, z_σ, through a logarithmic function ensures that $0 \le z_\sigma \le 1$. The functions $y^{\text{f}}(z_{\text{T}})$ and $y^{\text{r}}(z_{\text{T}})$ have the following expressions:

$$\begin{cases} y_{\text{T}}^{\text{f}}(z_{\text{T}}) = c^{\text{f}} z_{\text{T}} \\ y_{\text{T}}^{\text{r}}(z_{\text{T}}) = Y_{T0}^{\text{r}} + \bar{\sigma} + c^{\text{r}}(1 - z_{\text{T}}) \end{cases} \tag{16}$$

with $\bar{\sigma} = \sqrt{\frac{3}{2}\boldsymbol{s} : \boldsymbol{s}}$, while c^{f}, c^{r} and Y_{T0}^{r} are material parameters.

3 Finite strain constitutive model

In this section, we move from the constitutive model reviewed in Sect. 2 and using a multiplicative decomposition of the deformation gradient into elastic and inelastic parts, along with an additive decomposition of the inelastic strain rate tensor into transformation and reorientation parts, we derive a finite strain constitutive model.

3.1 Preliminaries

Considering a deformable body, we denote with $\boldsymbol{F}$ the deformation gradient and with J its determinant, supposed to be positive. The right and left Cauchy–Green deformation tensors are then, respectively, defined as:

$$\boldsymbol{C} = \boldsymbol{F}^{\mathrm{T}}\boldsymbol{F}, \quad \boldsymbol{b} = \boldsymbol{F}\boldsymbol{F}^{\mathrm{T}} \tag{17}$$

and the Green–Lagrange strain tensor $\mathbf{E}$ reads as:

$$\boldsymbol{E} = \frac{\boldsymbol{C} - \mathbf{1}}{2}. \tag{18}$$

Moreover, the velocity gradient tensor $\boldsymbol{l}$ is given as:

$$\boldsymbol{l} = \dot{\boldsymbol{F}}\boldsymbol{F}^{-1}. \tag{19}$$

The symmetric and anti-symmetric parts of $\boldsymbol{l}$ supply the strain rate tensor $\boldsymbol{d}$ and the vorticity $\boldsymbol{w}$, that is:

$$\boldsymbol{d} = \frac{1}{2}\left(\boldsymbol{l} + \boldsymbol{l}^{\mathrm{T}}\right), \quad \boldsymbol{w} = \frac{1}{2}\left(\boldsymbol{l} - \boldsymbol{l}^{\mathrm{T}}\right). \tag{20}$$

Taking the time derivative of Eq. (18) and using (17) and (20), it can be shown that:

$$\dot{\boldsymbol{E}} = \boldsymbol{F}^{\mathrm{T}}\boldsymbol{d}\boldsymbol{F}. \tag{21}$$

Finally, the second Piola–Kirchhoff stress tensor $\boldsymbol{S}$ is obtained from the Cauchy stress as:

$$\boldsymbol{S} = J\boldsymbol{F}^{-1}\boldsymbol{\sigma}\boldsymbol{F}^{-\mathrm{T}}. \tag{22}$$

3.2 Finite deformation formulation of constitutive model

Following a well-established approach adopted in plasticity [53,54] and already used for SMAs [9,34–40], we assume a local multiplicative decomposition of the deformation gradient into an elastic part $\boldsymbol{F}^{\mathrm{e}}$, defined with respect to an intermediate configuration, and an inelastic one $\boldsymbol{F}^{\mathrm{in}}$, defined with respect to the reference configuration. Accordingly:

$$\boldsymbol{F} = \boldsymbol{F}^{\mathrm{e}}\boldsymbol{F}^{\mathrm{in}}. \tag{23}$$

Since experimental evidences indicate that the inelastic flow is nearly isochoric, we have to impose $\det\left(\boldsymbol{F}^{\mathrm{in}}\right) = 1$, which after taking the time derivative results in:

$$\mathrm{tr}\left(\boldsymbol{d}^{\mathrm{in}}\right) = 0, \tag{24}$$

where $\boldsymbol{d}^{\mathrm{in}} = \mathrm{sym}(\dot{\boldsymbol{F}}^{\mathrm{in}}\boldsymbol{F}^{\mathrm{in}})$. We define $\boldsymbol{C}^{\mathrm{e}} = \boldsymbol{F}^{\mathrm{e}\,\mathrm{T}}\boldsymbol{F}^{\mathrm{e}}$ and $\boldsymbol{C}^{\mathrm{in}} = \boldsymbol{F}^{\mathrm{in}\,\mathrm{T}}\boldsymbol{F}^{\mathrm{in}}$ as the elastic and the inelastic right Cauchy–Green deformation tensors and using definitions (17) and (23), we obtain:

$$\boldsymbol{C}^{\mathrm{e}} = \boldsymbol{F}^{\mathrm{in}^{-\mathrm{T}}}\boldsymbol{C}\boldsymbol{F}^{\mathrm{in}^{-1}}. \tag{25}$$

Analogously to (2), we also define the stress-induced martensite fraction as [38–40]:

$$z_\sigma = \frac{\|\boldsymbol{E}^{\rm in}\|}{\varepsilon_{\rm L}}, \tag{26}$$

where $\varepsilon_{\rm L} = \sqrt{\frac{3}{2}}\gamma$ is a material parameter.

In order to satisfy the principle of material objectivity, the Helmholtz free energy has to depend on $\boldsymbol{F}^{\rm e}$ only through the elastic right Cauchy–Green deformation tensor; it is moreover assumed to be a function of the stress- and temperature-induced martensite fractions and the temperature in the following form [38–40]:

$$\Psi = \Psi\left(\boldsymbol{C}^{\rm e}, z_\sigma, z_{\rm T}, T\right) = \frac{1}{\rho_0} W\left(\boldsymbol{C}^{\rm e}\right) + \psi\left(z_\sigma, z_{\rm T}, T\right), \tag{27}$$

where ρ_0 is the reference density and $W(\boldsymbol{C}^{\rm e})$ is a hyperelastic strain energy function. In addition, we assume $W(\boldsymbol{C}^{\rm e})$ to be an isotropic function of $\boldsymbol{C}^{\rm e}$ and to be the same for austenite and martensite phases; it can be therefore expressed as:

$$W(\boldsymbol{C}^{\rm e}) = W\left(\mathrm{I}_{\boldsymbol{C}^{\rm e}}, \mathrm{II}_{\boldsymbol{C}^{\rm e}}, \mathrm{III}_{\boldsymbol{C}^{\rm e}}\right), \tag{28}$$

where $\mathrm{I}_{\boldsymbol{C}^{\rm e}}$, $\mathrm{II}_{\boldsymbol{C}^{\rm e}}$, $\mathrm{III}_{\boldsymbol{C}^{\rm e}}$ are the invariants of $\boldsymbol{C}^{\rm e}$. We also define ψ in the following form [21]:

$$\begin{aligned} \psi\left(z_\sigma, z_{\rm T}, T\right) = u_0^{\rm A} - T\eta_0^{\rm A} - z_{\rm T}\left(\Delta u_0 - T\Delta\eta_0\right) + z_\sigma\left\langle T\Delta\eta_0 - \Delta u_0\right\rangle \\ + c_v\left[(T - T_0) - T\ln\left(\frac{T}{T_0}\right)\right] + \frac{1}{2}H_\sigma z_\sigma^2 \end{aligned} \tag{29}$$

where the meaning of the material parameters is the same as in Sect. 2.

Taking the time derivative of Eq. 25 and using (19), the material time derivative of the elastic right Cauchy–Green deformation tensor is obtained as:

$$\dot{\boldsymbol{C}}^{\rm e} = -\boldsymbol{l}^{{\rm in}^{\rm T}}\boldsymbol{C}^{\rm e} + \boldsymbol{F}^{{\rm in}^{-\rm T}}\dot{\boldsymbol{C}}\boldsymbol{F}^{{\rm in}^{-1}} - \boldsymbol{C}^{\rm e}\boldsymbol{l}^{\rm in}. \tag{30}$$

According to (26), the time derivative of the stress-induced martensite fraction is given as:

$$\dot{z}_\sigma = \frac{\boldsymbol{E}^{\rm in}}{\boldsymbol{\varepsilon}_{\bf L}\|\boldsymbol{E}^{\rm in}\|} : \dot{\boldsymbol{E}}^{\rm in}, \tag{31}$$

where $\dot{\boldsymbol{E}}^{\rm in}$ is expressed as (see (21)):

$$\dot{\boldsymbol{E}}^{\rm in} = \boldsymbol{F}^{{\rm in}^{\rm T}}\boldsymbol{d}^{\rm in}\boldsymbol{F}^{\rm in}. \tag{32}$$

Substituting (32) into (31) and using the relations $\boldsymbol{C}^{\rm in} = \boldsymbol{F}^{{\rm in}^{\rm T}}\boldsymbol{F}^{\rm in}\boldsymbol{b}^{\rm in} = \boldsymbol{F}^{\rm in}\boldsymbol{F}^{{\rm in}^{\rm T}}$ and $\boldsymbol{E}^{\rm in} = (\boldsymbol{C}^{\rm in} - \mathbf{1})/2$, we obtain:

$$\dot{z}_\sigma = \frac{\boldsymbol{F}^{\rm in}\boldsymbol{E}^{\rm in}\boldsymbol{F}^{{\rm in}^{\rm T}}}{\varepsilon_{\rm L}\|\boldsymbol{E}^{\rm in}\|} : \boldsymbol{d}^{\rm in} = \frac{\boldsymbol{b}^{{\rm in}^2} - \boldsymbol{b}^{\rm in}}{2\varepsilon_{\rm L}\|\boldsymbol{E}^{\rm in}\|} : \boldsymbol{d}^{\rm in} \tag{33}$$

where we have also used the classical property of second-order tensor double contraction, $\boldsymbol{A} : (\boldsymbol{B}\boldsymbol{C}) = \boldsymbol{B} : (\boldsymbol{A}\boldsymbol{C}^{\rm T}) = \boldsymbol{C} : (\boldsymbol{B}^{\rm T}\boldsymbol{A})$.

We now decompose additively $\boldsymbol{d}^{\rm in}$ into a component $\boldsymbol{d}^{\rm tr}$ coaxial with $(\boldsymbol{b}^{{\rm in}^2} - \boldsymbol{b}^{\rm in})^{\rm D}$ and a component $\boldsymbol{d}^{\rm re}$ normal to $(\boldsymbol{b}^{{\rm in}^2} - \boldsymbol{b}^{\rm in})^{\rm D}$, where the superscript D indicates the deviator of a tensor ($\boldsymbol{A}^{\rm D} = \boldsymbol{A} - \frac{1}{3}({\rm tr}\boldsymbol{A})\mathbf{1}$), that is:

$$\boldsymbol{d}^{\rm in} = \boldsymbol{d}^{\rm tr} + \boldsymbol{d}^{\rm re} \tag{34}$$

with

$$\boldsymbol{d}^{\rm tr} = \left(\boldsymbol{d}^{\rm in} : \bar{\boldsymbol{H}}\right)\bar{\boldsymbol{H}}, \quad \boldsymbol{d}^{\rm re} = \boldsymbol{d}^{\rm in} - \left(\boldsymbol{d}^{\rm in} : \bar{\boldsymbol{H}}\right)\bar{\boldsymbol{H}} \tag{35}$$

and

$$\bar{\boldsymbol{H}} = \frac{\left(\boldsymbol{b}^{\text{in}2} - \boldsymbol{b}^{\text{in}}\right)^{\text{D}}}{\left\| \left(\boldsymbol{b}^{\text{in}2} - \boldsymbol{b}^{\text{in}}\right)^{\text{D}} \right\|}. \tag{36}$$

Using (24) and (35), we may also conclude that

$$\text{tr}(\boldsymbol{d}^{\text{tr}}) = 0, \quad \text{tr}(\boldsymbol{d}^{\text{re}}) = 0 \tag{37}$$

which is consistent with the experimental evidences of (nearly) isochoric conditions under forward and reverse transformation, as well as during reorientation.
Combining (33) and (34), we obtain

$$\dot{z}_\sigma = \frac{\boldsymbol{b}^{\text{in}2} - \boldsymbol{b}^{\text{in}}}{2\varepsilon_{\text{L}} \left\| \boldsymbol{E}^{\text{in}} \right\|} : \left(\boldsymbol{d}^{\text{tr}} + \boldsymbol{d}^{\text{re}}\right) = \frac{\left(\boldsymbol{b}^{\text{in}2} - \boldsymbol{b}^{\text{in}}\right)^{\text{D}}}{2\varepsilon_{\text{L}} \left\| \boldsymbol{E}^{\text{in}} \right\|} : \left(\boldsymbol{d}^{\text{tr}} + \boldsymbol{d}^{\text{re}}\right). \tag{38}$$

According to (35), the $\boldsymbol{d}^{\text{re}}$ component does not contribute to the variation of martensite fraction, but only produces a reorientation of the inelastic strain according to the local stress state and consequently, it can be considered as the reorientation part of $\boldsymbol{d}^{\text{in}}$, while the component $\boldsymbol{d}^{\text{tr}}$ can be considered as the transformation part.[3]

In this way, Eq. 38 reduces to

$$\dot{z}_\sigma = \frac{\left(\boldsymbol{b}^{\text{in}2} - \boldsymbol{b}^{\text{in}}\right)^{\text{D}}}{2\varepsilon_{\text{L}} \left\| \boldsymbol{E}^{\text{in}} \right\|} : \boldsymbol{d}^{\text{tr}} = \frac{\boldsymbol{b}^{\text{in}2} - \boldsymbol{b}^{\text{in}}}{2\varepsilon_{\text{L}} \left\| \boldsymbol{E}^{\text{in}} \right\|} : \boldsymbol{d}^{\text{tr}}. \tag{39}$$

Now we use the Clausius–Duhem inequality form of the second law of thermodynamics:

$$\frac{1}{\rho_0} \boldsymbol{S} : \dot{\boldsymbol{E}} - \left(\dot{\Psi} + \eta \dot{T}\right) \geq 0 \tag{40}$$

Substituting (27) into (40), after multiplication by ρ_0, we obtain

$$\boldsymbol{S} : \frac{1}{2}\dot{\boldsymbol{C}} - \frac{\partial W}{\partial \boldsymbol{C}^{\text{e}}} : \dot{\boldsymbol{C}}^{\text{e}} - \rho_0 \frac{\partial \psi}{\partial z_\sigma} \dot{z}_\sigma - \rho_0 \frac{\partial \psi}{\partial z_{\text{T}}} \dot{z}_{\text{T}} - \rho_0 \left(\eta + \frac{\partial \psi}{\partial T}\right) \dot{T} \geq 0. \tag{41}$$

Thus, substituting (30) and (39) into (41), after some mathematical manipulations, we obtain:

$$\begin{aligned} &\left(\boldsymbol{S} - 2\boldsymbol{F}^{\text{in}-1} \frac{\partial W}{\partial \boldsymbol{C}^{\text{e}}} \boldsymbol{F}^{\text{in}-\text{T}}\right) : \frac{1}{2}\dot{\boldsymbol{C}} - \rho_0 \left(\eta + \frac{\partial \psi}{\partial T}\right) \dot{T} \\ &+ \left(\frac{\partial W}{\partial \boldsymbol{C}^{\text{e}}} \boldsymbol{C}^{\text{e}} + \boldsymbol{C}^{\text{e}} \frac{\partial W}{\partial \boldsymbol{C}^{\text{e}}}\right) : \boldsymbol{l}^{\text{in}} - \rho_0 \frac{\partial \psi}{\partial z_\sigma} \frac{\boldsymbol{b}^{\text{in}2} - \boldsymbol{b}^{\text{in}}}{2\varepsilon_{\text{L}} \left\| \boldsymbol{E}^{\text{in}} \right\|} : \boldsymbol{d}^{\text{tr}} - \rho_0 \frac{\partial \psi}{\partial z_{\text{T}}} \dot{z}_{\text{T}} \geq 0. \end{aligned} \tag{42}$$

We now use the isotropic property of $W(\boldsymbol{C}^{\text{e}})$, implying that $\boldsymbol{C}^{\text{e}}$ and $\dfrac{\partial W}{\partial \boldsymbol{C}^{\text{e}}}$ are coaxial, that is:

$$\frac{\partial W}{\partial \boldsymbol{C}^{\text{e}}} \boldsymbol{C}^{\text{e}} = \boldsymbol{C}^{\text{e}} \frac{\partial W}{\partial \boldsymbol{C}^{\text{e}}}. \tag{43}$$

Substituting (43) into (42), we obtain:

$$\begin{aligned} &\left(\boldsymbol{S} - 2\boldsymbol{F}^{\text{in}-1} \frac{\partial W}{\partial \boldsymbol{C}^{\text{e}}} \boldsymbol{F}^{\text{in}-\text{T}}\right) : \frac{1}{2}\dot{\boldsymbol{C}} - \rho_0 \left(\eta + \frac{\partial \psi}{\partial T}\right) \dot{T} + 2\boldsymbol{C}^{\text{e}} \frac{\partial W}{\partial \boldsymbol{C}^{\text{e}}} : \boldsymbol{l}^{\text{in}} - \rho_0 \frac{\partial \psi}{\partial z_\sigma} \frac{\boldsymbol{b}^{\text{in}2} - \boldsymbol{b}^{\text{in}}}{2\varepsilon_{\text{L}} \left\| \boldsymbol{E}^{\text{in}} \right\|} : \boldsymbol{d}^{\text{tr}} \\ &- \rho_0 \frac{\partial \psi}{\partial z_{\text{T}}} \dot{z}_{\text{T}} \geq 0. \end{aligned} \tag{44}$$

[3] This interpretation makes clear the reason for the name choice of the coaxial and normal components as, respectively, $\boldsymbol{d}^{\text{tr}}$ and $\boldsymbol{d}^{\text{re}}$.

Following standard arguments, we finally conclude that:

$$\begin{cases} \boldsymbol{S} = 2\boldsymbol{F}^{\mathrm{in}^{-1}} \dfrac{\partial W}{\partial \boldsymbol{C}^{\mathrm{e}}} \boldsymbol{F}^{\mathrm{in}^{-\mathrm{T}}} \\ \eta = -\dfrac{\partial \psi}{\partial T} \end{cases} \tag{45}$$

and

$$\boldsymbol{M} : \boldsymbol{d}^{\mathrm{in}} - \boldsymbol{N} : \boldsymbol{d}^{\mathrm{tr}} + X_{\mathrm{T}} \dot{z}_{\mathrm{T}} \geq 0 \tag{46}$$

where

$$\begin{cases} \boldsymbol{M} = 2\boldsymbol{C}^{\mathrm{e}} \dfrac{\partial W}{\partial \boldsymbol{C}^{\mathrm{e}}} \\ \boldsymbol{N} = \rho_0 \dfrac{\partial \psi}{\partial z_\sigma} \dfrac{\boldsymbol{b}^{\mathrm{in}^2} - \boldsymbol{b}^{\mathrm{in}}}{2\varepsilon_{\mathrm{L}} \left\| \boldsymbol{E}^{\mathrm{in}} \right\|} = \rho_0 \left[\langle T \Delta \eta_0 - \Delta u_0 \rangle + H_\sigma z_\sigma \right] \dfrac{\boldsymbol{b}^{\mathrm{in}^2} - \boldsymbol{b}^{\mathrm{in}}}{2\varepsilon_{\mathrm{L}} \left\| \boldsymbol{E}^{\mathrm{in}} \right\|} \\ X_{\mathrm{T}} = -\rho_0 \dfrac{\partial \psi}{\partial z_{\mathrm{T}}} = -\rho_0 \left(T \Delta \eta_0 - \Delta u_0 \right). \end{cases} \tag{47}$$

Combining Eqs. 46 and 34, the dissipation inequality can be written as:

$$\boldsymbol{M} : \boldsymbol{d}^{\mathrm{re}} + (\boldsymbol{M} - \boldsymbol{N}) : \boldsymbol{d}^{\mathrm{tr}} + X_{\mathrm{T}} \dot{z}_{\mathrm{T}} \geq 0. \tag{48}$$

3.3 Evolution equations

In order to satisfy the second law of thermodynamics (48), we may define the following evolution equations:

$$\begin{cases} \boldsymbol{d}^{\mathrm{tr}} = \dot{\lambda}_{\mathrm{tr}} (\boldsymbol{M} - \boldsymbol{N})^{\mathrm{D}} \\ \boldsymbol{d}^{\mathrm{re}} = \dot{\lambda}_{\mathrm{re}} \tilde{\bar{\mathbb{I}}} : \boldsymbol{M}^{\mathrm{D}} \\ \dot{z}_{\mathrm{T}} = \dot{\lambda}_{\mathrm{T}} X_{\mathrm{T}} \end{cases} \tag{49}$$

where the fourth order tensor $\tilde{\bar{\mathbb{I}}}$ is defined as:

$$\tilde{\bar{\mathbb{I}}} = \mathbb{I} - \bar{\boldsymbol{H}} \otimes \bar{\boldsymbol{H}}. \tag{50}$$

We note that definition $(49)_2$ toghether with (50) ensures that $\boldsymbol{d}^{\mathrm{re}} : \bar{\boldsymbol{H}} = 0$.

In order to describe phase transformation, reorientation and twinned martensite evolutions, we choose three limit functions F_{tr}, F_{re} and F_{T} as:

$$\begin{aligned} F_{\mathrm{tr}} &= \|(\boldsymbol{M} - \boldsymbol{N})^{\mathrm{D}}\| - Y_{\mathrm{tr}}(z_\sigma) \\ F_{\mathrm{re}} &= \tfrac{1}{2} \boldsymbol{M}^{\mathrm{D}} : \tilde{\bar{\mathbb{I}}} : \boldsymbol{M}^{\mathrm{D}} - Y_{\mathrm{re}} \\ F_{\mathrm{T}} &= \begin{cases} X_{\mathrm{T}} - Y_{\mathrm{T}}^{\mathrm{f}}(z_{\mathrm{T}}) & \text{if } \dot{z}_{\mathrm{T}} > 0 \\ -X_{\mathrm{T}} - Y_{\mathrm{T}}^{\mathrm{r}}(z_{\mathrm{T}}) & \text{if } \dot{z}_{\mathrm{T}} < 0 \end{cases} \end{aligned} \tag{51}$$

where Y_{re} is a material parameter controlling the reorientation process, while $Y_{\mathrm{tr}}(z_\sigma)$ is a function governing the kinetics of the phase transformation. We assume functions $Y_{\mathrm{tr}}(z_\sigma)$ and $Y_{\mathrm{T}}^{\mathrm{f}}(z_{\mathrm{T}})$ to have the same form as in the SSF (see (15) and (16_1)). Moreover, we assume the following form for $Y_{\mathrm{T}}^{\mathrm{r}}$:

$$Y_{\mathrm{T}}^{\mathrm{r}}(z_{\mathrm{T}}) = Y_{T0}^{\mathrm{r}} + \tilde{\sigma} + c^{\mathrm{r}}(1 - z_{\mathrm{T}}) \tag{52}$$

with $\tilde{\sigma} = \sqrt{\frac{3}{2}(\boldsymbol{J}\boldsymbol{s}) : (\boldsymbol{J}\boldsymbol{s})}$.

Similarly to plasticity, the consistency parameters and the limit functions satisfy the Kuhn–Tucker conditions:

$$\begin{aligned} &F_{\mathrm{tr}} \leq 0, \quad \dot{\lambda}_{\mathrm{tr}} \geq 0, \quad \dot{\lambda}_{\mathrm{tr}} F_{\mathrm{tr}} = 0 \\ &F_{\mathrm{re}} \leq 0, \quad \dot{\lambda}_{\mathrm{re}} \geq 0, \quad \dot{\lambda}_{\mathrm{re}} F_{\mathrm{re}} = 0 \\ &F_{\mathrm{T}} \leq 0, \quad \dot{\lambda}_{\mathrm{T}} \geq 0, \quad \dot{\lambda}_{\mathrm{T}} F_{\mathrm{T}} = 0. \end{aligned} \tag{53}$$

We stress that, in order to reproduce the asymmetric behavior in tension and compression shown by SMAs in many experiments (see, e.g., [55,56]), different choices for limit functions should be introduced (see, e.g., [39] among others). However, this issue is beyond the purpose of the present article and such an enhancement will be considered in future works.

3.4 Representation with respect to the reference configuration

In the previous section, using a multiplicative decomposition of the deformation gradient into elastic and inelastic parts, we derived a finite strain constitutive model for SMAs. However, while $\boldsymbol{F}$ and $\boldsymbol{F}^{\text{in}}$ are related to the reference configuration, $\boldsymbol{F}^{\text{e}}$ has been defined with respect to an intermediate configuration. It is, however, necessary to recast all equations in terms of quantities described with respect to the reference configuration, so that all quantities are Lagrangian.

Since a hyperelastic strain energy function $W(\boldsymbol{C}^{\text{e}})$ has been introduced in terms of $\boldsymbol{C}^{\text{e}}$ (i.e. with respect to the intermediate configuration), we first investigate it.

As introduced in (28), W depends on $\boldsymbol{C}^{\text{e}}$ only through its invariants. However, the invariants of $\boldsymbol{C}^{\text{e}}$ are equal to those of $\boldsymbol{C}\boldsymbol{C}^{\text{in}^{-1}}$, as we show for the first invariant (the same can be shown also for the second and the third invariants in a similar way):

$$I_{\boldsymbol{C}^{\text{e}}} = \text{tr}\left(\boldsymbol{C}^{\text{e}}\right) = \text{tr}\left(\boldsymbol{F}^{\text{in}^{-\text{T}}}\boldsymbol{C}\boldsymbol{F}^{\text{in}^{-1}}\right) = \text{tr}\left(\boldsymbol{C}\boldsymbol{F}^{\text{in}^{-1}}\boldsymbol{F}^{\text{in}^{-T}}\right) = \text{tr}\left(\boldsymbol{C}\boldsymbol{C}^{\text{in}^{-1}}\right) = I_{\boldsymbol{C}\boldsymbol{C}^{\text{in}^{-1}}}. \tag{54}$$

Since we assumed W to be an isotropic function of $\boldsymbol{C}^{\text{e}}$, considering representation theorem it can be written in the following form [57]:

$$\frac{\partial W}{\partial \boldsymbol{C}^{\text{e}}} = \alpha_1 \mathbf{1} + \alpha_2 \boldsymbol{C}^{\text{e}} + \alpha_3 \boldsymbol{C}^{\text{e}2} \tag{55}$$

where $\alpha_i = \alpha_i(\text{I}_{\boldsymbol{C}\boldsymbol{C}^{\text{in}^{-1}}},\ \text{II}_{\boldsymbol{C}\boldsymbol{C}^{\text{in}^{-1}}},\ \text{III}_{\boldsymbol{C}\boldsymbol{C}^{\text{in}^{-1}}})$. Substituting (55) into (45) and using (25), we conclude that:

$$\boldsymbol{S} = 2\left(\alpha_1 \boldsymbol{C}^{\text{in}^{-1}} + \alpha_2 \boldsymbol{C}^{\text{in}^{-1}}\boldsymbol{C}\boldsymbol{C}^{\text{in}^{-1}} + \alpha_3 \boldsymbol{C}^{\text{in}^{-1}}\left(\boldsymbol{C}\boldsymbol{C}^{\text{in}^{-1}}\right)^2\right) \tag{56}$$

which expresses the second Piola–Kirchhoff stress tensor in terms of quantities computed with respect to the reference configuration.

In order to find the Lagrangian form of the tensorial evolution equation, we combine (49) with (34) and substituting it into (32), we obtain:

$$\dot{\boldsymbol{E}}^{\text{in}} = \boldsymbol{F}^{\text{in}^{\text{T}}}\left(\dot{\lambda}_{\text{tr}}\left(\boldsymbol{M}-\boldsymbol{N}\right)^{\text{D}} + \dot{\lambda}_{\text{re}}\tilde{\tilde{\mathbb{I}}} : \boldsymbol{M}^{\text{D}}\right)\boldsymbol{F}^{\text{in}} \tag{57}$$

or equivalently,

$$\dot{\boldsymbol{C}}^{\text{in}} = 2\dot{\lambda}_{\text{tr}}\boldsymbol{F}^{\text{in}^{\text{T}}}\left(\boldsymbol{M}-\boldsymbol{N}\right)^{\text{D}}\boldsymbol{F}^{\text{in}} + 2\dot{\lambda}_{\text{re}}\boldsymbol{F}^{\text{in}^{\text{T}}}\tilde{\tilde{\mathbb{I}}} : \boldsymbol{M}^{\text{D}}\boldsymbol{F}^{\text{in}}. \tag{58}$$

We now consider the first term in the definition of the tensorial internal variable in (58), which is related to the transformation. To this end we compute:

$$\boldsymbol{F}^{\text{in}^{\text{T}}}\boldsymbol{M}\boldsymbol{F}^{\text{in}} = (\boldsymbol{F}^{\text{in}}\boldsymbol{C}^{\text{e}}\boldsymbol{F}^{\text{in}})\left(\boldsymbol{F}^{\text{in}^{-1}} 2\frac{\partial W}{\partial \boldsymbol{C}^{\text{e}}}\boldsymbol{F}^{\text{in}^{-T}}\right)\boldsymbol{C}^{\text{in}} = \boldsymbol{C}\boldsymbol{S}\boldsymbol{C}^{\text{in}} \tag{59}$$

and

$$\boldsymbol{F}^{\text{in}^{\text{T}}}\boldsymbol{N}\boldsymbol{F}^{\text{in}} = \rho_0\frac{\partial \psi}{\partial z_\sigma}\frac{\boldsymbol{C}^{\text{in}^3} - \boldsymbol{C}^{\text{in}^2}}{2\varepsilon_{\text{L}}\left\|\boldsymbol{E}^{\text{in}}\right\|} = \boldsymbol{C}^{\text{in}}\left(\frac{\rho_0}{\varepsilon_{\text{L}}}\frac{\partial \psi}{\partial z_\sigma}\frac{\boldsymbol{E}^{\text{in}}}{\left\|\boldsymbol{E}^{\text{in}}\right\|}\right)\boldsymbol{C}^{\text{in}} = \boldsymbol{C}^{\text{in}}\boldsymbol{X}\boldsymbol{C}^{\text{in}} \tag{60}$$

where we have defined:

$$\boldsymbol{X} = \frac{\rho_0}{\varepsilon_{\text{L}}}\frac{\partial \psi}{\partial z_\sigma}\frac{\boldsymbol{E}^{\text{in}}}{\left\|\boldsymbol{E}^{\text{in}}\right\|}. \tag{61}$$

We now define:

$$\boldsymbol{Y}\boldsymbol{C}^{\text{in}} = \boldsymbol{F}^{\text{in}^{\text{T}}}(\boldsymbol{M}-\boldsymbol{N})\boldsymbol{F}^{\text{in}} \tag{62}$$

and obtain from (59)–(62) the asymmetric tensor $\boldsymbol{Y}$ as follows:

$$\boldsymbol{Y} = \boldsymbol{C}\boldsymbol{S} - \boldsymbol{C}^{\text{in}}\boldsymbol{X}. \tag{63}$$

Moreover, we have:

$$\begin{aligned}\boldsymbol{F}^{\text{in}^{\text{T}}}(\boldsymbol{M}-\boldsymbol{N})^{\text{D}}\boldsymbol{F}^{\text{in}} &= \boldsymbol{F}^{\text{in}^{\text{T}}}\left(\boldsymbol{M}-\boldsymbol{N}-\frac{1}{3}tr(\boldsymbol{M}-\boldsymbol{N})\boldsymbol{1}\right)\boldsymbol{F}^{\text{in}} \\ &= \left(\boldsymbol{C}\boldsymbol{S}\boldsymbol{C}^{\text{in}} - \boldsymbol{C}^{\text{in}}\boldsymbol{X}\boldsymbol{C}^{\text{in}} - \frac{1}{3}tr(\boldsymbol{C}\boldsymbol{S})\boldsymbol{C}^{\text{in}} + \frac{1}{3}tr(\boldsymbol{C}^{\text{in}}\boldsymbol{X})\boldsymbol{C}^{\text{in}}\right) = \boldsymbol{Y}^{\text{D}}\boldsymbol{C}^{\text{in}}\end{aligned} \tag{64}$$

yielding

$$(\boldsymbol{M}-\boldsymbol{N})^{\text{D}} = \boldsymbol{F}^{\text{in}^{-\text{T}}}\boldsymbol{Y}^{\text{D}}\boldsymbol{F}^{\text{in}^{\text{T}}} \tag{65}$$

and

$$(\boldsymbol{M}-\boldsymbol{N})^{\text{D}} : (\boldsymbol{M}-\boldsymbol{N})^{\text{D}^{\text{T}}} = \boldsymbol{Y}^{D} : \boldsymbol{Y}^{\text{D}^{\text{T}}} \qquad \text{or} \qquad \|(\boldsymbol{M}-\boldsymbol{N})^{\text{D}}\| = \|\boldsymbol{Y}^{\text{D}}\|. \tag{66}$$

The second term in the evolution Eq. 58 can be rewritten in a similar way as [58]:

$$\boldsymbol{F}^{\text{in}^{\text{T}}}(\tilde{\tilde{\mathbb{I}}} : \boldsymbol{M}^{\text{D}})\boldsymbol{F}^{\text{in}} = (\tilde{\mathbb{I}} : \boldsymbol{Z}^{\text{D}})\boldsymbol{C}^{\text{in}} \tag{67}$$

where

$$\boldsymbol{Z} = \boldsymbol{C}\boldsymbol{S} \tag{68}$$

$$\tilde{\mathbb{I}} = \mathbb{I} - \boldsymbol{H} \otimes \boldsymbol{H} \tag{69}$$

$$\boldsymbol{H} = \frac{(\boldsymbol{C}^{\text{in}^2} - \boldsymbol{C}^{\text{in}})^{\text{D}}}{\|(\boldsymbol{C}^{\text{in}^2} - \boldsymbol{C}^{\text{in}})^{\text{D}}\|}. \tag{70}$$

It can also be shown that [58]:

$$\boldsymbol{M}^{\text{D}} : \tilde{\tilde{\mathbb{I}}} : \boldsymbol{M}^{\text{D}} = \boldsymbol{Z}^{\text{D}} : \tilde{\mathbb{I}} : \boldsymbol{Z}^{\text{D}}. \tag{71}$$

Finally using (22), we obtain

$$(\boldsymbol{J}\boldsymbol{s}) : (\boldsymbol{J}\boldsymbol{s}) = \|(\boldsymbol{C}\boldsymbol{S})^{\text{D}}\|^2 \tag{72}$$

showing that in (52) we can express $\tilde{\sigma}$ in terms of quantities defined with respect to the reference configuration.

We are now ready to formulate the finite deformation constitutive model, written in terms of Lagrangian quantities only, which can be summarized as follows:

– Stress quantities

$$\begin{aligned}\boldsymbol{S} &= 2\left(\alpha_1\boldsymbol{C}^{\text{in}^{-1}} + \alpha_2\boldsymbol{C}^{\text{in}^{-1}}\boldsymbol{C}\boldsymbol{C}^{\text{in}^{-1}} + \alpha_3\boldsymbol{C}^{\text{in}^{-1}}(\boldsymbol{C}\boldsymbol{C}^{\text{in}^{-1}})^2\right) \\ \boldsymbol{Y} &= \boldsymbol{C}\boldsymbol{S} - \boldsymbol{C}^{\text{in}}\boldsymbol{X} \\ \boldsymbol{Z} &= \boldsymbol{C}\boldsymbol{S} \\ \boldsymbol{X} &= \rho_0\left[\langle T\Delta\eta_0 - \Delta u_0\rangle + H_\sigma z_\sigma\right]\frac{\boldsymbol{E}^{\text{in}}}{\|\boldsymbol{E}^{\text{in}}\|} \\ X_{\text{T}} &= -\rho_0\,(T\Delta\eta_0 - \Delta u_0)\end{aligned}$$

– Evolution equation

$$\begin{aligned}\dot{\boldsymbol{C}}^{\text{in}} &= \left(2\dot{\lambda}_{\text{tr}}\boldsymbol{Y}^{\text{D}} + 2\dot{\lambda}_{\text{re}}\tilde{\mathbb{I}} : \boldsymbol{Z}^{\text{D}}\right)\boldsymbol{C}^{\text{in}} \\ \dot{z}_{\text{T}} &= \dot{\lambda}_{\text{T}}X_{\text{T}}\end{aligned}$$

– Limit functions

$$\begin{aligned} F_{\mathrm{tr}} &= \|\boldsymbol{Y}^{\mathrm{D}}\| - Y_{\mathrm{tr}}(z_\sigma) \\ F_{\mathrm{re}} &= \tfrac{1}{2}\boldsymbol{Z}^{\mathrm{D}} : \tilde{\mathbb{I}} : \boldsymbol{Z}^{\mathrm{D}} - Y_{\mathrm{re}} \\ f_{\mathrm{T}} &= \begin{cases} X_{\mathrm{T}} - Y_{\mathrm{T}}^{\mathrm{f}}(z_{\mathrm{T}}) & \text{if } \dot{z}_{\mathrm{T}} > 0 \\ -X_{\mathrm{T}} - Y_{\mathrm{T}}^{\mathrm{r}}(z_{\mathrm{T}}) & \text{if } \dot{z}_{\mathrm{T}} < 0 \end{cases} \end{aligned}$$

– Kuhn–Tucker conditions

$$\begin{aligned} &F_{\mathrm{tr}} \le 0, \quad \dot{\lambda}_{\mathrm{tr}} \ge 0, \quad \dot{\lambda}_{\mathrm{tr}} F_{\mathrm{tr}} = 0 \\ &F_{\mathrm{re}} \le 0, \quad \dot{\lambda}_{\mathrm{re}} \ge 0, \quad \dot{\lambda}_{\mathrm{re}} F_{\mathrm{re}} = 0 \\ &F_{\mathrm{T}} \le 0, \quad \dot{\lambda}_{\mathrm{T}} \ge 0, \quad \dot{\lambda}_{\mathrm{T}} F_{\mathrm{T}} = 0 \end{aligned}$$

– Martensite volume fractions

$$z_\sigma = \frac{\|\boldsymbol{E}^{\mathrm{in}}\|}{\varepsilon_{\mathrm{L}}}, \quad 0 \le z_\sigma \le 1, \quad 0 \le z_{\mathrm{T}} \le 1, \quad 0 \le z_{\mathrm{T}} + z_\sigma \le 1.$$

Remark To be consistent with the small strain constitutive model development approach by Panico and Brinson, in this section, we used $\{\boldsymbol{C}^{\mathrm{e}}, T\}$ and $\{z_\sigma, z_{\mathrm{T}}\}$ as control and internal variables, respectively. However, we prefer to consider $\{\boldsymbol{C}, T\}$ and $\{\boldsymbol{C}^{\mathrm{in}}, z_{\mathrm{T}}\}$ as control and internal variables, respectively, as the final form of constitutive model confirms this. To this end, in Appendix A, we have developed finite strain constitutive model considering $\{\boldsymbol{C}, T\}$ as control variables as well as $\{\boldsymbol{C}^{\mathrm{in}}, z_{\mathrm{T}}\}$ as internal ones showing that both approaches lead to the same constitutive equations.

4 Linearization of the finite deformation SMA model

In this section, we derive the linearized form of the constitutive equations proposed in Sect. 3.4 and we compare it with the small strain constitutive model in [21]. The infinitesimal strain tensor is defined as:

$$\boldsymbol{\varepsilon} = \frac{1}{2}\left(\nabla\boldsymbol{u} + (\nabla\boldsymbol{u})^{\mathrm{T}}\right). \tag{73}$$

According to the definition of displacement vector, $\boldsymbol{u} = \boldsymbol{x} - \boldsymbol{X}$, we have:

$$\nabla\boldsymbol{u} = \boldsymbol{F} - \boldsymbol{1}. \tag{74}$$

Substituting $\boldsymbol{F}$ from (74) into (18), we find the relation between the Green–Lagrange strain tensor and the infinitesimal strain tensor as:

$$\boldsymbol{E} = \boldsymbol{\varepsilon} + \frac{1}{2}(\nabla\boldsymbol{u})^{\mathrm{T}}(\nabla\boldsymbol{u}). \tag{75}$$

Neglecting higher order terms, we then obtain the linearized form of kinematic quantities as

$$\begin{aligned} &\boldsymbol{E} \simeq \boldsymbol{\varepsilon}, \quad \boldsymbol{C} = \boldsymbol{1} + 2\boldsymbol{E} \simeq \boldsymbol{1} + 2\boldsymbol{\varepsilon} \\ &\boldsymbol{E}^{\mathrm{in}} \simeq \boldsymbol{\varepsilon}^{\mathrm{in}}, \quad \boldsymbol{C}^{\mathrm{in}} = \boldsymbol{1} + 2\boldsymbol{E}^{\mathrm{in}} \simeq \boldsymbol{1} + 2\boldsymbol{\varepsilon}^{\mathrm{in}} \\ &\boldsymbol{C}^{\mathrm{in}2} - \boldsymbol{C}^{\mathrm{in}} \simeq 2\boldsymbol{\varepsilon}^{\mathrm{in}}, \quad \boldsymbol{H} \simeq \boldsymbol{h}. \end{aligned} \tag{76}$$

Also, it can be shown that stress quantities have the following linearized form:

$$\begin{aligned} &\boldsymbol{S} \simeq tr\,(\boldsymbol{\varepsilon})\,\boldsymbol{\sigma} + O\,(\boldsymbol{\varepsilon}) = \frac{\rho_0}{\rho}\boldsymbol{\sigma} + O\,(\boldsymbol{\varepsilon}) \simeq \boldsymbol{\sigma} \\ &\boldsymbol{C}\boldsymbol{S} \simeq \boldsymbol{\sigma} \\ &\boldsymbol{X} \simeq \rho\frac{1}{\varepsilon_{\mathrm{L}}}\frac{\partial\psi}{\partial z_\sigma}\frac{\boldsymbol{\varepsilon}^{\mathrm{in}}}{\|\boldsymbol{\varepsilon}^{\mathrm{in}}\|} = \boldsymbol{x} \\ &\boldsymbol{Y}^{\mathrm{D}} \simeq \boldsymbol{s} - \boldsymbol{x} = \boldsymbol{x}_{\mathrm{tr}} \\ &\boldsymbol{Z}^{\mathrm{D}} \simeq \boldsymbol{s} = \boldsymbol{x}_{\mathrm{re}} \\ &X_{\mathrm{T}} = -\rho_0(T\Delta\eta_0 - \Delta u_0) \simeq x_{\mathrm{T}}. \end{aligned} \tag{77}$$

In finite elasticity, it is usually supposed that for a hyperelastic material, the strain energy function $W(\boldsymbol{C}^e)$ reduces to the strain energy of a hookean elastic material in the small strain regime [57]. Therefore, we may conclude that independently on the functional form of $W(\boldsymbol{C}^{\mathrm{e}})$ (e.g., Saint–Venant Kirchhoff type, Neo–Hookean, Mooney–Rivlin, Ogden, etc.), the linearized form reads as:

$$W \simeq \frac{1}{2}\lambda(\mathrm{tr}(\boldsymbol{\varepsilon}^{\mathrm{e}}))^2 + \mu\,\mathrm{tr}(\boldsymbol{\varepsilon}^{\mathrm{e}2}) \tag{78}$$

where λ and μ are Lamè constants.

Applying the linearized forms in (76)–(78) to the finite deformation constitutive model of Sect. 3 readily gives the same constitutive model proposed in [21].

5 Application of the proposed constitutive model to the simple shear test

In this section, we apply the proposed finite strain constitutive model to study the pseudo-elastic behavior of a SMA under simple shear test[4]. Analysis of the simple shear deformation has become a popular benchmark for testing the validity of finite deformation constitutive models. The reasonableness and applicability of various models has been investigated using this problem [59].
Up to now, all relations have been derived in a completely general manner without specifying the form of the strain energy function W, apart from the fact that it is supposed to be an isotropic function of $\boldsymbol{C}^e$. Despite the hyperelastic strain energy function W can take any well-known form in finite elasticity, for the example to be discussed in this section, we use the commonly used Saint–Venant–Kirchhoff strain energy function:

$$W = \frac{\lambda}{2}\left(\mathrm{tr}\boldsymbol{E}^{\mathrm{e}}\right)^2 + \mu\,\mathrm{tr}\boldsymbol{E}^{\mathrm{e}2} \tag{79}$$

which yields:

$$\alpha_1 = \frac{\lambda}{4}\left(\boldsymbol{C} : \boldsymbol{C}^{\mathrm{in}^{-1}} - 3\right) - \frac{1}{2}\mu, \qquad \alpha_2 = \frac{1}{2}\mu, \qquad \alpha_3 = 0 \tag{80}$$

where λ and μ are the Lamè constants.

The proposed model has 17 parameters, i.e. E and ν (elastic material parameters), γ, Δu_0, $\Delta\eta_0$ and H_σ (transformation related parameters), A^{f}, B^{f} and C^{f} (forward phase transformation related parameters), A^{r}, B^{r} and C^{r} (reverse phase transformation parameters), Y_{re} (reorientation parameter), c^{f}, Y^{r}_{T0} and c^{r} (temperature-induced phase transformation parameters) and ρ (material density). We refer the reader to [60] for a material parameter identification strategy. We use the material properties listed in Table 1, typical for Nitinol, and corresponding to characteristic temperatures: $M_{\mathrm{f}} = 306\,\mathrm{K}$, $M_{\mathrm{s}} = 310\,\mathrm{K}$, $A_{\mathrm{s}} = 317$ K and $A_{\mathrm{f}} = 319\,\mathrm{K}$ [21].

We start simulating a loading–unloading simple shear test (see Fig. 1a) at a temperatures $T = 360\,\mathrm{K}$ for which we expect a pseudo-elastic behavior. The deformation gradient is expressed in terms of the shear amount κ as follows:

$$\boldsymbol{F} = \begin{bmatrix} 1 & \kappa & 0 \\ 0 & 1 & 0 \\ 0 & 0 & 1 \end{bmatrix}. \tag{81}$$

Figure 1b, c, d presents the Cauchy stress components σ_{11}, σ_{12} and σ_{22}, respectively, in terms of the shear amount κ for both the SSF and the FSF. It is observed that the material recovers the original shape after unloading, reproducing a superelastic behavior for $T > A_{\mathrm{f}}$. According to the above-mentioned results, we conclude that, for small values of κ, the small and FSF yield nearly the same result, but the SSF deviation grows up by increasing the shear amount value. While, the σ_{12} component in both formulation is nearly the same (but deviation starts increasing for $\kappa > 0.14$), the σ_{11} and σ_{22} components are zero in SSF and rapidly

[4] We remark that, the aim of this section is to highlight the finite deformation effects; therefore, numerical investigation of the constitutive model features is not of interest.

Table 1 Material parameters adopted in the simple shear test [21].

Parameter	Value	Unit
E	68400	MPa
ν	0.36	–
γ	0.0612[a]	–
Δu_0	14725	J/Kg
$\Delta \eta_0$	47.5	J/Kg K
H_σ	100	J/Kg
ρ	8000	Kg/m^3
A^f	0	MPa
B^f	10	MPa
C^f	72.6	MPa
A^r	0	MPa
B^r	0	MPa
C^r	72.6	MPa
Y_{re}	50	MPa^2
c^f	190	J/Kg
Y^r_{T0}	2.66	MPa
c^r	95	J/Kg

[a] We use a larger value (more realistic) for this parameter than in [21]; the original value was 0.038.

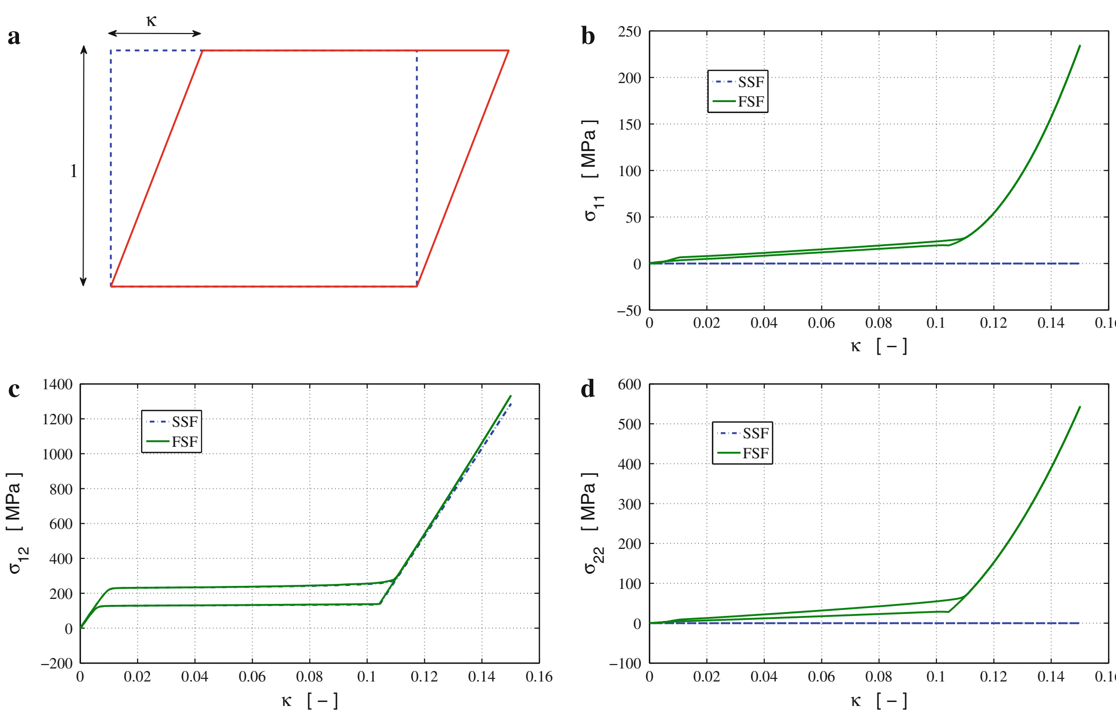

Fig. 1 Comparison of small (SSF) and finite (FSF) strain formulations under simple shear test: **a** deformation in a simple shear test; **b** σ_{11} component in terms of κ; **c** σ_{12} component in terms of κ; **d** σ_{22} component in terms of κ

increasing for $\kappa > 0.11$ in FSF. We stress that this deviation is not surprising, since the small strain constitutive model is based on the assumption hat the reference and current configurations are approximately the same, while for a large values of κ, this assumption is not valid.

This example simply shows the nonlinear geometry effects and highlights the necessity of using a finite deformation constitutive model for SMA-based structures in which usually large rotations and moderate strains are present.

6 Conclusions and Summary

The increasing number of shape memory alloy applications motivates the development of constitutive models to better predict material complex behaviors. On one hand, martensite reorientation is one of the most important features of SMAs, responsible for the specific response under non-proportional loadings. On the other hand, undergoing large rotations and moderate strains by SMA devices is an important issue in material behavior modeling. To this end, in this study, a 3D finite strain constitutive model is developed extending a recently proposed small strain model. A multiplicative decomposition of the deformation gradient into elastic and inelastic parts, in combination with an additive decomposition of the inelastic strain rate tensor into transformation and reorientation parts, is used within the framework of continuum thermodynamics with internal variables.

Implemented in a numerical scheme like, e.g. FEM, this constitutive model has the potential to constitute a reliable tool to simulate and design shape memory alloy devices and structures under complicate loading conditions. Numerical implementation of the model within FEM, as well as considering asymmetric behavior of material under tension and compression, will be the subject of future work.

Acknowledgements J. Arghavani has been partially supported by Iranian Ministry of Science, Research and Technology, and partially by Dipartimento di Meccanica Strutturale, Università degli Studi di Pavia. F. Auricchio and A. Reali have been partially supported by the Cariplo Foundation through the project number n.2009.2822; by the Ministero dell'Istruzione, dell'Università e della Ricerca through the project n. 2008MRKXLX; and by the European Research Council through the Starting Independent Research Grant "BioSMA: Mathematics for Shape Memory Technologies in Biomechanics".

Appendix A: finite strain constitutive model derivation considering $\boldsymbol{C}$ and T as control variables and $\boldsymbol{C}^{\text{in}}$ and z_{T} as internal ones

In Sect. 3, we considered $\{\boldsymbol{C}^{\text{e}} T\}$ and $\{z_\sigma z_{\text{T}}\}$ as control and internal variables, respectively. Here, we assume $\boldsymbol{C}$ and T as control variables as well as $\boldsymbol{C}^{\text{in}}$ and z_{T} as internal ones, which seems more realistic.

A hyperelastic strain energy function depends only on elastic deformation through $\boldsymbol{C}^{\text{e}}$ or according to (25) on $\boldsymbol{F}^{\text{in}^{-\text{T}}}\boldsymbol{C}\boldsymbol{F}^{\text{in}^{-1}}$. Now, applying the principle of objectivity, we obtain:

$$W(\boldsymbol{C}^{\text{e}}) = W\left(\boldsymbol{F}^{\text{in}^{-\text{T}}}\boldsymbol{C}\boldsymbol{F}^{\text{in}^{-1}}\right) = W\left(\boldsymbol{U}^{\text{in}^{-1}}\boldsymbol{C}\boldsymbol{U}^{\text{in}^{-1}}\right). \tag{82}$$

An isotropic strain energy function depends on $\boldsymbol{U}^{\text{in}^{-1}}\boldsymbol{C}\boldsymbol{U}^{\text{in}^{-1}}$ only through its invariants which are equal to those of $\boldsymbol{C}\boldsymbol{C}^{\text{in}^{-1}}$. Therefore, we assume W as a function of $\bar{\boldsymbol{C}} = \boldsymbol{C}\boldsymbol{C}^{\text{in}^{-1}}$ and define the Helmholtz free energy function in the following form:

$$\Psi\left(\boldsymbol{C}, T, \boldsymbol{C}^{\text{in}}, z_{\text{T}}\right) = \frac{1}{\rho_0} W(\boldsymbol{C}\boldsymbol{C}^{\text{in}^{-1}}) + \psi(\boldsymbol{C}^{\text{in}}, z_{\text{T}}, T) \tag{83}$$

where ψ is defined as (29) while z_σ substituted by $\dfrac{\|\boldsymbol{C}^{\text{in}} - \mathbf{1}\|}{2\varepsilon_{\text{L}}}$ (see Eq. 26).
Substituting (83) in Clausius–Duhem inequality (40), we obtain:

$$\left(\boldsymbol{S} - 2\frac{\partial W}{\partial \boldsymbol{C}}\right) : \frac{1}{2}\dot{\boldsymbol{C}} - \frac{\partial W}{\partial \boldsymbol{C}^{\text{in}}} : \dot{\boldsymbol{C}}^{\text{in}} - \rho_0 \frac{\partial \psi}{\partial \boldsymbol{C}^{\text{in}}} : \dot{\boldsymbol{C}}^{\text{in}} - \rho_0 \frac{\partial \psi}{\partial z_{\text{T}}}\dot{z}_{\text{T}} - \rho_0\left(\eta + \frac{\partial \psi}{\partial T}\right)\dot{T} \geq 0. \tag{84}$$

Using some mathematical manipulations, we also obtain following relations [58]:

$$\begin{cases} \dfrac{\partial W}{\partial \boldsymbol{C}} = \boldsymbol{C}^{\text{in}^{-1}}\left(\dfrac{\partial W}{\partial \bar{\boldsymbol{C}}}\right)^{\text{T}} \\ \dfrac{\partial W}{\partial \boldsymbol{C}^{\text{in}}} = \boldsymbol{C}^{\text{in}}\left(\dfrac{\partial W}{\partial \bar{\boldsymbol{C}}}\right)^{\text{T}} \boldsymbol{C}\boldsymbol{C}^{\text{in}^{-1}}. \end{cases} \tag{85}$$

Substituting (85) into (84), using (21) and following standard arguments, we obtain:

$$\begin{cases} \boldsymbol{S} = 2\boldsymbol{C}^{\text{in}^{-1}} \left(\dfrac{\partial W}{\partial \bar{\boldsymbol{C}}}\right)^{\text{T}} \\ \eta = -\dfrac{\partial \psi}{\partial T} \end{cases} \tag{86}$$

and

$$\bar{\boldsymbol{M}} : \boldsymbol{d}^{\text{in}} - \bar{\boldsymbol{N}} : \boldsymbol{d}^{\text{tr}} + X_{\text{T}} \dot{z}_{\text{T}} \geq 0 \tag{87}$$

where

$$\begin{cases} \bar{\boldsymbol{M}} = 2\boldsymbol{F}^{\text{in}^{-\text{T}}} \boldsymbol{C} \dfrac{\partial W}{\partial \bar{\boldsymbol{C}}} \boldsymbol{F}^{\text{in}^{-1}} \\ \bar{\boldsymbol{N}} = 2\boldsymbol{F}^{\text{in}} \rho_0 \dfrac{\partial \psi}{\partial \boldsymbol{C}^{\text{in}}} \boldsymbol{F}^{\text{in}^{\text{T}}} \end{cases} \tag{88}$$

and X_{T} has already been defined in $(47)_3$.

We may now write:

$$\frac{\partial W}{\partial \bar{\boldsymbol{C}}} = \alpha_1 \mathbf{1} + \alpha_2 \bar{\boldsymbol{C}}^{\text{T}} + \alpha_3 \left(\bar{\boldsymbol{C}}^2\right)^{\text{T}} \tag{89}$$

where $\alpha_i = \alpha_i(\text{I}_{\boldsymbol{C}\boldsymbol{C}^{\text{in}^{-1}}},\ \text{II}_{\boldsymbol{C}\boldsymbol{C}^{\text{in}^{-1}}},\ \text{III}_{\boldsymbol{C}\boldsymbol{C}^{\text{in}^{-1}}})$. Substituting (89) into (86) and (88) and following a similar approach used in Sect. 3, we obtain the same constitutive equations as summarized in Sect. 3.4.

References

1. Otsuka, K., Wayman, C.M.: Shape Memory Materials. Cambridge University Press, Cambridge (1998)
2. Duerig, T.W., Melton, K.N., Stoekel, D., Wayman, C.M.: Engineering Aspects of Shape Memory Alloys. Butterworth-Heinemann, London (1990)
3. Van Humbeeck, J.: Non-medical applications of shape memory alloys. Mater. Sci. Eng. A **273**(275), 134–148 (1999)
4. Duerig, T., Pelton, A., Stockel, D.: An overview of nitinol medical applications. Mater. Sci. Eng. A **273**(275), 149–160 (1999)
5. Kuribayashi, K., Tsuchiya, K., You, Z., Tomus, D., Umemoto, M., Ito, T. Sasaki M.: Self-deployable origami stent grafts as a biomedical application of Ni-rich TiNi shape memory alloy foil. Mater. Sci. Eng. A **419**(1–2), 131–137 (2006)
6. Funakubo, H.: Shape Memory Alloys. Gordon and Breach Science Publishers, New York (1987)
7. Lim, T.J., McDowell, D.L.: Mechanical behavior of an Ni-Ti shape memory alloy under axial-torsional proportional and nonproportional loading. J. Eng. Mater. Technol. **121**, 9–18 (1999)
8. Sittner, P., Hara, Y., Tokuda, M.: Experimental study on the thermoelastic martensitic transformation in shape memory alloy polycrystal induced by combined external forces. Metall. Mater. Trans. A **26**, 2923–2935 (1995)
9. Helm D.: Formgedächtnislegierungen–experimentelle untersuchung, phänomenologische modellierung und numerische simulation der thermomechanischen materialeigenschaften. Ph.D. thesis, Universitat Gesamthochschule Kassel (2001)
10. Helm D., Haupt P.: Thermomechanical representation of the multiaxial behavior of shape memory alloys. In: Lynch, C.S. (Ed.), Proceedings of SPIE Smart Structures and Materials 2002: Active Materials: Behavior and Mechanics, vol. 4699, pp. 343–354 (2002)
11. Bouvet, C., Calloch, S., Lexcellent, C.: Mechanical behavior of a Cu-Al-Be shape memory alloy under multiaxial proportional and nonproportional loadings. J. Eng. Mater. Technol. **124**, 112–124 (2002)
12. Grabe, C., Bruhns, O.: Path dependence and multiaxial behavior of a polycrystalline niti alloy within the pseudoelastic and pseudoplastic temperature regimes. Int. J. Plast. **25**, 513–545 (2009)
13. Patoor, E., Lagoudas, D.C., Entchev, P.B., Brinson, L.C., Gao, X.: Shape memory alloys, part I: general properties and modeling of single crystals. Mech. Mater. **38**(5-6), 391–429 (2006)
14. Lagoudas, D.C., Entchev, P.B., Popov, P., Patoor, E., Brinson, L.C., Gao, X.: Shape memory alloys, part II: modeling of polycrystals. Mech. Mater. **38**(5–6), 430–462 (2006)
15. Leclercq, S., Lexcellent, C.: A general macroscopic description of the thermomechanical behavior of shape memory alloys. J. Mech. Phys. Solids **44**(6), 953–957 (1996)
16. Bekker, A., Brinson, L.C.: Temperature-induced phase transformation in a shape memory alloy: Phase diagram based kinetics approach. J. Mech. Phys. Solids **45**(6), 949–988 (1987)
17. Bondaryev, E.N., Wayman, C.M.: Some stress–strain–temperature relationships for shape memory alloys. Metall. Trans. A **19A**(10), 2407–2413 (1988)
18. Chi, Y., Pence, T.J., Tsai, H.: Axisymmetric plane stress states of an annulus subject to displacive phase transformation. J. Appl. Mech. **72**, 44–53 (2005)

19. Chi, Y., Pence, T.J., Tsai, H.: Numerical algorithms for cyclic phase transformation hysteresis in a shape memory plate subject to axisymmetric plane stress. Int. J. Numer. Methods Eng. **69**, 1819–1850 (2007)
20. Raniecki, B., Lexcellent, C.: Thermodynamics of isotropic pseudoelasticity in shape memory alloys. Eur. J. Mech A/Solids **17**(2), 185–205 (1998)
21. Panico, M., Brinson, L.: A three-dimensional phenomenological model for martensite reorientation in shape memory alloys. J. Mech. Phys. Solids **55**(11), 2491–2511 (2007)
22. Arghavani J., Auricchio F., Naghdabadi R., Reali A., Sohrabpour S.: A 3-D phenomenological constitutive model for shape memory alloys under multiaxial loadings. Int. J. Plast. **26**, 976–991 (2010)
23. Souza, A.C., Mamiya, E.N., Zouain, N.: Three-dimensional model for solids undergoing stress-induced phase transformations. Eur. J. Mech. A/Solids **17**(5), 789–806 (1998)
24. Qidwai, M.A., Lagoudas, D.C.: Numerical implementation of a shape memory alloy thermomechanical constitutive model using return mapping algorithms. Int. J. Numer. Methods Eng. **47**, 1123–1168 (2000)
25. Brocca, M., Brinson, L.C., Bazant, Z.P.: Three-dimensional constitutive model for shape memory alloys based on microplane model. J. Mech. Phys. Solids **50**(5), 1051–1077 (2002)
26. Helm, D., Haupt, P.: Shape memory behaviour: modelling within continuum thermomechanics. Int. J. Solids Struct **40**(4), 827–849 (2003)
27. Auricchio, F., Marfia, S., Sacco, E.: Modelling of SMA materials: training and two way memory effects. Comput Struct **81**(24–25), 2301–2317 (2003)
28. Bouvet, C., Calloch, S., Lexcellent, C.: A phenomenological model for pseudoelasticity of shape memory alloys under multiaxial proportional and nonproportional loadings. Eur. J. Mech. A/Solids **23**(1), 37–61 (2004)
29. Lagoudas, D.C., Entchev, P.B.: Modeling of transformation-induced plasticity and its effect on the behavior of porous shape memory alloys. Part I: constitutive model for fully dense smas. Mech. Mater. **36**(9), 865–892 (2004)
30. Auricchio, F., Reali, A., Stefanelli, U.: A three-dimensional model describing stress-induced solid phase transformation with permanent inelasticity. Int. J. Plast. **23**(2), 207–226 (2007)
31. Popov, P., Lagoudas, D.C.: A 3-D constitutive model for shape memory alloys incorporating pseudoelasticity and detwinning of self-accommodated martensite. Int. J. Plast. **23**(10–11), 1679–1720 (2007)
32. Thiebaud, F., Lexcellent, C., Collet, M., Foltete, E.: Implementation of a model taking into account the asymmetry between tension and compression, the temperature effects in a finite element code for shape memory alloys structures calculations. Comput. Mater. Sci. **41**(2), 208–221 (2007)
33. Moumni, Z., Zaki, W., Nguyen, Q.S.: Theoretical and numerical modeling of solid-solid phase change: application to the description of the thermomechanical behavior of shape memory alloys. Int. J. Plast. **24**(4), 614–645 (2008)
34. Auricchio, F., Taylor, R.L.: Shape-memory alloys: modelling and numerical simulations of the finite-strain superelastic behavior. Comput. Methods Appl. Mech. Eng. **143**(1-2), 175–194 (1997)
35. Auricchio, F.: A robust integration-algorithm for a finite-strain shape-memory-alloy superelastic model. Int. J. Plast. **17**, 971–990 (2001)
36. Pethö, A.: Constitutive modelling of shape memory alloys at finite strain. Z. Angew. Math. Mech **81**(S2), 355–356 (2001)
37. Ziolkowski, A.: Three-dimensional phenomenological thermodynamic model of pseudoelasticity of shape memory alloys at finite strains. Contin. Mech. Thermodyn. **19**, 379–398 (2007)
38. Reese, S., Christ, D.: Finite deformation pseudo-elasticity of shape memory alloys—constitutive modelling and finite element implementation. Int. J. Plast. **24**(3), 455–482 (2008)
39. Christ, D., Reese, S.: A finite element model for shape memory alloys considering thermomechanical couplings at large strains. Int. J. Solids Struct. **46**(20), 3694–3709 (2009)
40. Evangelista V., Marfia S., Sacco E.: A 3D SMA constitutive model in the framework of finite strain. Int. J. Numer. Methods Eng. doi:10.1002/nme.2717 (2009)
41. Arghavani J., Auricchio F., Naghdabadi R., Reali A., Sohrabpour S.: On the robustness and efficiency of integration algorithms for a 3D finite strain phenomenological SMA constitutive model. Int. J. Numer. Methods Eng. doi:10.1002/nme.2964
42. Müller, C., Bruhns, O.: A thermodynamic finite-strain model for pseudoelastic shape memory alloys. Int. J. Plast. **22**(9), 1658–1682 (2006)
43. Bernardini, D., Pence, T.J.: A Multifield Theory for the Modeling of the Macroscopic Behavior of Shape Memory Materials. In: Advances in Multifield Theories for Continua with Substructure. Birkhauser, Boston (2004)
44. Raniecki, B., Lexcellent, C.: R_L-models of pseudoelasticity and their specifications for some shape memory alloys. Eur. J. Mech. A/Solids **13**(1), 21–50 (1994)
45. Auricchio, F., Petrini, L.: A three-dimensional model describing stress-temperature induced solid phase transformations: thermomechanical coupling and hybrid composite applications. Int. J. Numer. Methods Eng. **61**(5), 716–737 (2004)
46. Levitas, V.I.: Thermomechanical theory of martensitic phase transformations in inelastic materials. Int. J. Solids Struct. **35**, 889–940 (1998)
47. Idesman, A.V., Levitas, V.I., Stein, E.: Elastoplastic materials with martensitic phase transition and twinning at finite strains: numerical solution with finite element method. Comput. Methods Appl. Mech. Eng. **173**, 71–98 (1999)
48. Thamburaja, P., Anand, L.: Polycrystalline shape-memory materials: effect of crystallographic texture. J. Mech. Phys. Solids **49**, 709–737 (2001)
49. Thamburaja, P.: Constitutive equations for martensitic reorientation and detwinning in shape-memory alloys. J. Mech. Phys. Solids **53**, 825–856 (2005)
50. Stupkiewicz, S., Petryk, H.: Finite-strain micromechanical model of stress-induced martensitic transformations in shape memory alloys. Mater. Sci. Eng. A **438**(440), 126–130 (2006)
51. Pan, H., Thamburaja, P., Chau, F.S.: Multi-axial behavior of shape-memory alloys undergoing martensitic reorientation and detwinning. Int. J. Plast. **23**(4), 711–732 (2007)
52. Stein, E., Sagar, G.: Theory and finite element computation of cyclic martensitic phase transformation with finite strain. Int. J. Numer. Methods Eng. **74**, 1–31 (2008)

53. Lubarda, V.A.: Elastoplasticity Theory. CRC Press LLC, (2001)
54. Haupt, P.: Continuum Mechanics and Theory of Materials. Springer Publication House, New York (2001)
55. Liu, Y., Xie, Z.L., Van Humbeeck, J., Delaey, L.: Asymmetry of stress-strain curves under tension and compression for NiTi shape memory alloys. Acta Mater. **46**, 4325–4338 (1998)
56. Liu, Y., Xie, Z.L., Van Humbeeck, J., Delaey, L.: Effect of texture orientation on the martensite deformation of NiTi shape memory alloy sheet. Acta Mater. **47**, 645–660 (1999)
57. Ogden, R.W.: Non-linear Elastic Deformations. Ellis Horwood Limited, Chichester (1984)
58. Arghavani J.: Thermomechanical behavior of shape memory alloys under nonproportional loading: constitutive modelling and numerical inplementation in small and finite strains, Ph.d. Thesis, Sharif University of Technology, Iran (2010)
59. Yeganeh, Y., Naghdabadi, R.: Axial effects investigation in fixed-end circular bars under torsion with a finite deformation model based on logarithmic strain. Int. J. Mech. Sci. **48**(1), 75–84 (2006)
60. Auricchio, F., Coda, A., Reali, A., Urbano, M.: SMA numerical modeling versus experimental results: parameter identification and model prediction capabilities. J. Mater. Eng. Perform. **18**(5–6), 649–654 (2009)